

Color Printer Characterization Using a Computational Geometry Approach

Jon Yngve Hardeberg and Francis Schmitt

*École Nationale Supérieure des Télécommunications, Département Images,
Paris, France*

Abstract

We propose a method for the colorimetric characterization of a printer which can also be applied to any other type of digital image reproduction device. The method is based on a computational geometry approach. It uses a 3D triangulation technique to build a tetrahedral partition of the printer color gamut volume and it generates a surrounding structure enclosing the definition domain. The characterization provides the inverse transformation from the device-independent color space CIELAB to the device-dependent color space CMY, taking into account both colorimetric properties of the printer, and color gamut mapping.

1. Introduction

The characterization of a color output device such as a digital color printer defines the relationship between the device color space and a device-independent color space, typically based on CIE colorimetry. This relationship defines a (forward) printer model. Several approaches to printer modeling exist in the literature. They may be divided into two main groups:

- **Physical models.** Such models are based on knowledge of the physical or chemical behavior of the printing system, and are thus inherently dependent on the technology used (ink jet, dye sublimation, etc.). An important example of physical models for halftone devices is the Neugebauer model,¹ which treats the printed color as an additive mixture of the tristimulus values of the paper, the primary colors, and any overlap of primary colors. More recent applications of analytical modeling are illustrated with a study of Berns² which applies a modified version of the Kubelka-Munk spectral model to a dye diffusion thermal transfer printer.
- **Empirical models.** Such models do not explicitly require knowledge of the physical properties of the printer as they rely only on the measurement of a large number of color samples, used either to optimize a set of linear equations based on regression

algorithms, or to build lookup-tables for 3D interpolation. Regression models have not been found very successful in printer modeling,³ while the lookup-table method is used by several authors, for example Hung³ and Balasubramanian.⁴

However, both these groups of printer models have to be inverted to be of practical use for image reproduction. The solution to the inverse problem is difficult to find. Iterated optimization algorithms are often needed to determine the device color coordinates which reproduce a given color defined in a device-independent color space.

Another issue which cannot be avoided when discussing printer characterization is gamut mapping. The color gamut of a device such as a printer is defined as the range of colors that can be reproduced with this device. Gamut mapping is needed whenever two imaging devices do not have coincident color gamuts, in particular when a given color in the original document cannot be reproduced with the printer that is used. Numerous algorithms have been proposed.^{5,6,7} Gamut mapping techniques may be divided into two categories, *i*) **continuous methods** applied to all the colors of an image, such as gamut compression and white point adaptation, and *ii*) **clipping methods**, applied only to colors that are out of gamut. An efficient practical solution is likely to be a combination of these two categories.

We propose a characterization technique which provides a practical tool to transform any point of the CIELAB space into its corresponding CMY values. This process also includes a color gamut mapping technique which can be of any type. We use an approach based on computational geometry with which we construct two 3D structures which cover both the entire definition domain of the CIELAB space and the printer color gamut. It provides us with a partition of the space into two sets of non-intersecting tetrahedra, an **inner structure** covering the printer gamut, and a **surrounding structure**, the union of these two structures covering the entire definition domain of the CIELAB space. These 3D structures allow us to easily determine if a CIELAB point is inside or outside the printer color gamut, to apply a gamut mapping technique when necessary, and then to compute by non-regular tetrahedral

interpolation the corresponding CMY values. We establish thus an empirical inverse printer model. In the next section we describe the proposed method.

2. Methodology

Our method consists of first printing a numerical color chart (the input data) covering the entire color gamut of the printer to be characterized. Then we analyze colorimetrically the printed chart to obtain the CIELAB values corresponding to each sample. This analysis can be done with either *i*) a desktop scanner properly calibrated,⁸ or *ii*) a colorimeter, or better, *iii*) a spectrophotometer if available. Brettel *et al.*⁹ propose a versatile spectrophotometer for this purpose. When this is done, we dispose of the CIELAB values, and the corresponding CMY values, for each color sample of the chart. Storing these values in a lookup-table, we could thus easily establish an empirical forward printer model using interpolation techniques.^{3, 4}

The main step of the proposed printer characterization is the construction of a valid partition of the CIELAB space. A naive approach to this problem would be to apply a Delaunay triangulation directly to the measured CIELAB values. However, this would not suit our purpose, mainly because the gamut is generally not a convex hull in the CIELAB space, thus the gamut boundaries would not be correctly represented. In particular, any concavities of the gamut surface would be filled, and the information about the gamut surface would be lost. One solution to this problem would be to use a constrained triangulation preserving the gamut surface. But this would require the introduction of Steiner points for which efficient algorithms do not exist.¹⁰ We propose in the next section an indirect approach where we apply a 3D Delaunay triangulation in CMY space, which provides us with an inner structure of the cubic CMY color gamut. We then transport the resulting structure into CIELAB space. To cope with out-of-gamut colors we also propose the construction of a surrounding structure, as described in the following section. We then resume how the transformation from CIELAB to CMY is performed. This is followed by a presentation of how different gamut mapping techniques may be effectuated using the inner and surrounding structures.

2.1. Inner structure

First, from the set of CMY values corresponding to the color samples of the chart, we construct a 3D Delaunay triangulation^{10,11} in CMY space by taking the CMY triplets from the input data as vertices. Note that by using a Delaunay triangulation we are not limited to using colors lying on a regular grid in CMY space, as is the case with regular triangulation techniques such as those proposed by

Nin *et al.*¹² and Motomura *et al.*¹³ This implies that we can use colors that are more regularly distributed in CIELAB space, and that we can add more colors in regions where they are sparse or where the eye is more sensitive, for example grays or skin tones.

Using this 3D triangulation, we would be able to calculate the corresponding CIELAB values for a given CMY triplet simply by barycentric interpolation of the CIELAB values of the vertices of the tetrahedron surrounding the CMY triplet, as was also proposed by Bell and Cowan.¹⁴ This would provide us with a forward printer model. But we are indeed more interested in the inverse printer model. We thus transport the CMY triangulation into CIELAB space by simply replacing the CMY vertices of the triangulation by their measured CIELAB counterparts. This corresponds to a geometric deformation of the triangulation of the gamut cube in which the external boundaries are preserved, as shown in Figure 1. The resulting triangulation is no more a Delaunay triangulation in CIELAB space, the "empty circumsphere" criterion¹¹ being no longer fulfilled. But, it remains generally a valid partition of the CIELAB color gamut in the sense that a nonempty intersection of two transformed tetrahedra remains limited to a common face, edge or vertex. However, this must be verified since errors may occur due to either *i*) a too fine subdivision of the gamut, *ii*) measurement errors, or *iii*) strange behavior of either the printer driver software or the physical or chemical properties of the printer itself. If errors occur, some points of the input data may have to be eliminated from the triangulation. This verification can be easily effectuated by checking if a tetrahedron has been mirrored during the geometric deformation.

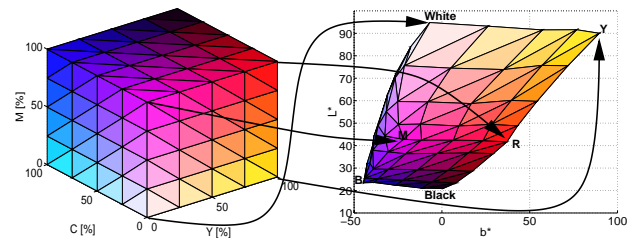


Figure 1: Triangulated CMY color gamut cube (left) and its corresponding geometrically deformed CIELAB color gamut (right).

2.2. Surrounding structure

At this point we dispose of an inner structure partitioning in tetrahedra the region of the CIELAB space lying inside the printer color gamut. We are able to calculate for any CIELAB color point of the gamut its corresponding CMY values by tetrahedral interpolation of the CMY values associated with the vertices.

In order to be able to treat out-of-gamut colors, we have added a surrounding structure in CIELAB space, defined by a set of fictive points as shown in Figure 2. The key issue here is the definition of this surrounding structure in such a way that, together with the inner structure, it defines a valid triangulation which includes the definition domain of the CIELAB space.

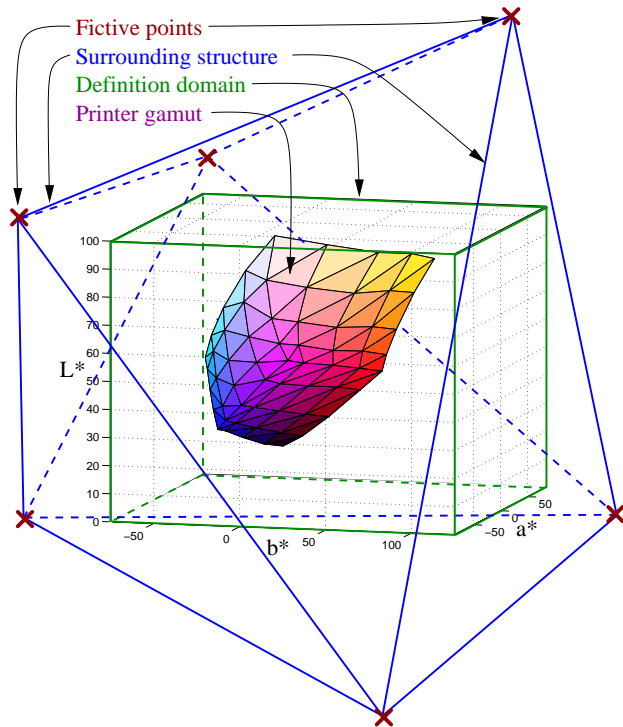


Figure 2: Octahedron surrounding the printer color gamut and the definition domain in CIELAB space.

We choose in CIELAB space a set of 6 fictive points, associated with the 6 faces of the gamut. These points are determined by computational geometry techniques so that they respect the following two criteria: *i*) each fictive point 'sees' the outer side of all triangles of its associated face, and *ii*) the convex hull defined by the fictive points (an octahedron) encloses the definition domain, as shown in Figure 2.

The practical realization of these external tetrahedra is performed using Delaunay triangulation in CMY space. That is, we define another set of 6 fictive points in CMY space as indicated in Figure 3 and we triangulate the joint set of fictive points and input data. Thus we construct three distinct classes of external tetrahedra, having 1, 2, or 3 vertices being fictive points, and the other vertices being color points belonging to the surface of the gamut cube, as shown in Figure 3. We then transport the resulting triangulation to CIELAB space by replacing the CMY vertices (fictive points and input data) with their CIELAB counter-

parts, as described in the previous section. We thus define a valid triangulation of the joint inner and surrounding structures in CIELAB space.

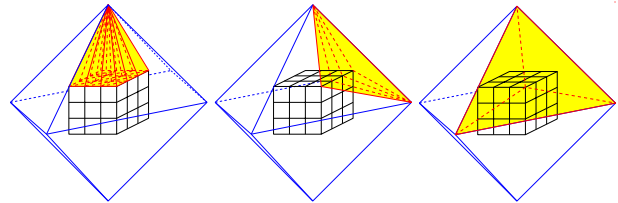


Figure 3: Surrounding structure in CMY space. The 3 classes of external tetrahedra are indicated.

2.3. CIELAB-to-CMY transformation

This 3D triangulation allows us then to calculate, by tetrahedral interpolation, the transformation from CIELAB to CMY values for any point belonging to the definition domain of CIELAB space. This is typically done either *i*) directly for all pixels of an image to be printed, or *ii*) for all the vertices of a regular grid composing a CIELAB-to-CMY 3D lookup-table which can be stored in a device profile and further used by a color management system (CMS).^{8,15}

The tetrahedron \mathcal{T}^P that encloses the input CIELAB point P is located using a 'walking' algorithm. If \mathcal{T}^P belongs to the surrounding structure, then P is an out-of-gamut point. A gamut clipping technique using the 3D structures is then applied to identify a new point P' that belongs to the gamut surface as described in the next section.

When the tetrahedron with vertices $P_0P_1P_2P_3$ belonging to the color gamut and enclosing the point P (or P' when P is out of gamut) is found, the resulting CMY values are calculated by barycentric interpolation as follows: P (or P') divides the enclosing tetrahedron into 4 sub-tetrahedrons, each having a volume determined by the following determinant:

$$\Delta_i = \frac{1}{6} \begin{vmatrix} P_{i+1} & P_{i+2} & P_{i+3} & P \\ 1 & 1 & 1 & 1 \end{vmatrix}, \quad i = 0 \dots 3,$$

where the indices are taken modulo 3, and finally, the barycentric coefficients W_i are defined by $W_i = \Delta_i/\Delta$, where Δ is the volume of the tetrahedron $P_0P_1P_2P_3$.

The final output values C , M , and Y are then calculated as follows:

$$C = \sum_{i=0}^3 W_i C_{P_i}, \quad M = \sum_{i=0}^3 W_i M_{P_i}, \quad Y = \sum_{i=0}^3 W_i Y_{P_i}$$

where C_{P_i} , M_{P_i} , and Y_{P_i} are the CMY values associated with the tetrahedron vertices $P_i, i = 0 \dots 3$.

2.4. Gamut mapping

The 3D structures allow us to implement easily any gamut mapping technique, such as those mentioned in the introduction. Our geometrical approach is particularly well adapted to a combination of continuous and clipping methods.

When needed, a continuous gamut mapping technique may be applied to each input point prior to the interpolation described above. However, if the inverse gamut mapping function exists, it is more computationally effective to apply it to the CIELAB vertices of the 3D structures, as shown for the case of a simple compression in Figure 4. The advantage of this approach is to directly include the gamut mapping transformation into the localization step of the input point in the 3D structures. However, here also we must verify that no tetrahedron is mirrored during the inverse gamut mapping transformation in order to preserve a valid triangulation in CIELAB space. Other continuous gamut mapping techniques such as a 3D morphing¹⁶ can also be applied.

If, after the continuous gamut mapping, the input color point is still out of gamut, that is, \mathcal{T}^P belongs to the surrounding structure as already discussed in the previous section, a gamut clipping method must be applied. For example a radial clipping¹⁷ is easily effectuated by 'walking' from tetrahedron to tetrahedron, following a line from P towards a mid-gamut point until a tetrahedron belonging to the gamut is encountered.

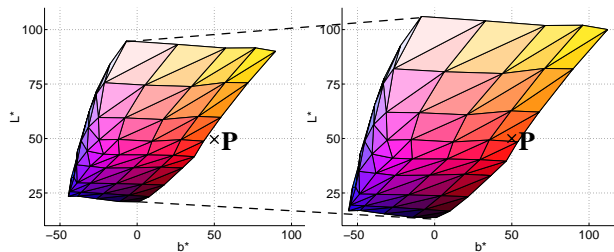


Figure 4: A gamut compression of 20% performed by applying the inverse compression onto all the vertices of the 3D structures (only the inner structure is represented here).

3. Conclusion

The proposed printer characterization method presents several strong points of interest. First, it performs efficiently the inverse transformation from CIELAB (or any other 3D color space) to CMY directly without using numerical optimization techniques. Secondly it is able to easily incorporate different gamut mapping techniques, both continuous and clipping methods. Thirdly it is versatile, not being

limited to one specific printing technology. The extension to fourcolor CMYK printers is straightforward when the amount of black ink is determined directly from the CMY values as in the gray-component replacement¹ (GCR) technique.

4. References

1. H. R. Kang. *Color Technology for Electronic Imaging Devices*. SPIE Optical Engineering Press, 1997.
2. R. S. Berns. *Spectral modeling of a dye diffusion thermal transfer printer*. Tech. rep., Munsell Color Science Laboratory, 1993.
3. P.-C. Hung. "Colorimetric calibration in electronic imaging devices using a look-up-table method and interpolations". *J. Electronic Imaging*, 2(1):53-61, 1993.
4. R. Balasubramanian. "Color transformations for printer color correction". In *Proc. IS&T and SID's 2nd Color Imaging Conference: Color Science, Systems and Applications*, pp.62-65, 1994.
5. M. C. Stone, W. B. Cowan, and J. C. Beatty. "Color gamut mapping and the printing of digital color images". *ACM Trans. on Graphics*, 7(4):249-292, 1988.
6. L. W. MacDonald. "Gamut mapping in perceptual colour space". In *Proc. IS&T and SID's Color Imaging Conference: Transforms and Transportability of Color*, pp.193-196, 1993.
7. M. Wolski, J. P. Allebach, and C. A. Bouman. "Gamut mapping. Squeezing the most out of your color system". In *Proc. IS&T and SID's 2nd Color Imaging Conference: Color Science, Systems and Applications*, pp.89-92, 1994.
8. J. Y. Hardeberg, F. Schmitt, I. Tastl, H. Brettel, and J.-P. Crettez. "Color management for color facsimile". In *Proc. IS&T and SID's 4th Color Imaging Conf.: Color Science, Systems and Applications*, pp.108-113, 1996.
9. H. Brettel, A. Chiron, J. Y. Hardeberg, and F. Schmitt. "Versatile spectrophotometer for cross-media color management". In *AIC Color 97*, Kyoto, Japan, 1997.
10. M. Bern and D. Eppstein. "Mesh generation and optimal triangulation". In *Computing in Euclidean Geometry*, pp.23-90. World Scientific Publishing, 2. ed., 1992.
11. S. Fortune. "Voronoi diagrams and Delaunay triangulations". In *Computing in Euclidean Geometry*, pp. 193-233. World Scientific Publishing, 2. ed., 1992.
12. S. I. Nin, J. M. Kasson, and W. Plouffe. "Printing CIELAB images on a CMYK printer using tri-linear interpolation". In *SPIE Proc., Color Hard Copy and Graphic Arts*, 1670:316-324, 1992.
13. H. Motomura, T. Fumoto, O. Yamada, K. Kanamori, and H. Kotera. "CIELAB to CMYK color conversion by prism and slant prism interpolation method". In *Proc. IS&T and SID's 2nd Color Imaging Conference: Color Science, Systems and Applications*, pp.156-159, 1994.
14. I. E. Bell and W. Cowan. "Characterizing printer gamuts using tetrahedral interpolation". In *Proc. IS&T and SID's Color Imaging Conference: Transforms and Transportability of Color*, pp.108-113, 1993.
15. *ICC Profile Format Specification*. The International Color Consortium, 1996. Version 3.3, <ftp://sgigate.sgi.com/pub/icc/ICC33.pdf>.
16. K. E. Spaulding, R. N. Ellson, and J. R. Sullivan. "Ultra-Color: A new gamut mapping strategy". In *SPIE Proc. Device Independent Color Imaging II*, 2414:61-68, 1995.
17. E. G. Pariser. "An investigation of color gamut reduction techniques". In *Proc. IS&T Symp. on Electr. Prepress Technology - Color Printing*, pp.105-107, 1991.